Linear dynamics of elastic Helical springs: Asymptotic analysis of wave propagation

Article *in* Proceedings of The Royal Society A · March 2009

DOI: 10.1098/rspa.2008.0468

1 author:

S.V. Sorokin
Aalborg University
99 PUBLICATIONS **803** CITATIONS

SEE PROFILE

PROCEEDINGS OF THE ROYAL SOCIETY A MATHEMATICAL, PHYSICAL & ENGINEERING SCIENCES

Linear dynamics of elastic helical springs: asymptotic analysis of wave propagation

S.V. Sorokin

Proc. R. Soc. A 2009 **465**, doi: 10.1098/rspa.2008.0468 first published online 25 February 2009

PROCEEDINGS OF THE ROYAL SOCIETY A

Proc. R. Soc. A (2009) **465**, 1513–1537
doi:10.1098/rspa.2008.0468
Published online 25 February 2009

Linear dynamics of elastic helical springs: asymptotic analysis of wave propagation

By S. V. Sorokin*

Department of Mechanical Engineering, Aalborg University, Pontoppidanstraede 101, 9220 Aalborg, Denmark

Helical springs serve as vibration isolators in virtually any suspension system. A variety of theories to describe the dynamic behaviour of these structural elements, which involves interaction of flexural, torsion and longitudinal waves, can be found in the literature. Alongside this, various approximate methods are employed to determine the eigenfrequencies of vibrations of springs. In this paper, the validity ranges of alternative theories are assessed by comparison of the location of the dispersion curves. This paper also contains a rigorous asymptotic analysis of the exact dispersion equation with two small parameters being employed. It allows for the identification of significant regimes of linear wave motion in a helical spring. In each of these regimes, simple formulae for wavenumbers are obtained by the dominant balance method and their validity ranges are checked against direct numerical solution. Mode shapes associated with each wavenumber are also analysed.

Keywords: helical spring; wave propagation; asymptotic analysis

1. Introduction

Helical springs are used in virtually all suspension systems and they serve as vibration isolators. It is obvious that modelling of springs as idealized elements having no mass and frequency-independent stiffness is applicable only in quasi-static cases, and then the excitation frequency is markedly lower than the first eigenfrequency of their vibrations.

It is not surprising that the analysis of linear vibrations of springs has received much attention starting from the classical treatment by Love (1899). Several alternative theories, some of those being simpler, while others being more complicated than Love's, have been formulated in the literature. The diversity of models is explained by the complexity of the exact (in the framework of rod theory) equations and by significant difficulties with their analytical solution. It is perhaps more surprising that, to the best of the author's knowledge, no effort seems to have been made to perform asymptotic analysis of these equations, which could be helpful to gain a physical understanding of dynamic phenomena for the vibrations of springs in various regimes of excitation. It also seems that the location of dispersion curves has been studied in just a few references.

*svs@ime.aau.dk

Received 17 November 2008
Accepted 21 January 2009

The main objectives of the present paper may be summarized in the following way. First of all, it is reasonable to assess the accuracy of existing simplified theories. Naturally, this assessment may be performed in various ways, but the most robust one is based on the comparison of locations of all branches of dispersion curves (complex-valued, purely real and purely imaginary). The solution of the three-dimensional problem in elastodynamics is the natural reference for such an assessment—exactly as the Rayleigh–Lamb solution of the problem of wave propagation in an elastic layer is used to assess validity ranges of elementary theories of straight beams. However, this paper is concerned with wave propagation in a helical spring at relatively low frequencies and the reference is chosen as Timoshenko-type theory, which incorporates shear deformation and rotary inertia as was formulated by Wittrick (1966). As long as all branches of dispersion curves are adequately described by any reduced theory, there is no reason to employ this one.

The second goal is to perform asymptotic analysis of the dispersion equation and to identify the significant regimes of wave propagation in a spring. To accomplish this task, it is necessary to take into account that the equations of motion of a helical spring involve two small parameters, namely the ratio of the diameter of a wire to the radius of a spring and the pitch angle. Once these regimes of wave propagation are identified and asymptotic formulae for all wavenumbers are available via setting dominant balances, it is possible to analyse the associated eigenmodes.

Studies of linear wave motion in helical springs are naturally continued by tackling the problem of calculation of eigenfrequencies of springs of a finite length. Although this task may be accomplished by the standard dynamic stiffness matrix method, far more numerically stable results can be obtained by the implementation of the boundary integral equation method. The superiority of this method in comparison with others is ensured because Green's matrix for an infinitely long spring, which satisfies radiation and decay conditions, is employed. It naturally paves the way for the analysis of forced vibrations of a spring in arbitrary excitation conditions, but this step lies beyond the scope of this paper. Obviously, a formulation of Green's matrix would also facilitate the analysis of energy transmission in a spring, which involves all types of deformation—axial, torsion and flexural—in proportions strongly dependent upon the excitation conditions. This aspect is also left out of the scope of this paper.

The brief literature survey reported in the remaining part of this section encompasses two subjects: the level of approximation of theoretical model of a helical spring and the analysis of waveguide properties of a helical spring. Numerous publications on dynamics of planar curved beams are summarized, for example, by Chidamparam & Leissa (1993).

As regards theoretical models, virtually all of them are based on the 'plane cross-section' approximation, which is standard in the theory of elastic rods. Recently, a helical spring has been treated in the framework of three-dimensional elastodynamics by Treysséde (2008). This author has employed a semi-analytical finite-element method to study wave propagation in a spring with a large pitch. The Timoshenko-type theory has been introduced by Wittrick (1966) and used by Mottershead (1980), Yildirim (1996), Lee & Thompson (2001), Becker *et al.* (2002), Telem *et al.* (2004) and Lee (2007). Simplification of this model by neglecting rotary inertia and shear deformation is a standard way to proceed

from the Timoshenko model to the classical Bernoulli–Euler model. However, in the literature (see Wittrick 1966; Pearson & Wittrick 1986), the Bernoulli–Euler model is introduced with an additional assumption that deformation due to axial load may be neglected. As is shown in §2, this simplification is dangerous because it dramatically narrows the frequency range, where this 'standard' model is adequate. Therefore, all other models, which attempt to advance with further simplifications (e.g. 'lateral vibration of a spring' or 'axial vibration of a spring'; see Phillips & Costello 1972; Guido *et al.* 1978; Jiang *et al.* 1992), may not qualify to be used as a tool to accurately predict waveguide properties of helical spring in arbitrary excitation conditions.

An analysis of dispersion curves for a reduced model of spring has been performed by Guido *et al.* (1978), whereas the general Timoshenko-type theory has been treated by Lee & Thompson (2001) and Lee (2007). Although the exact formulation of dispersion equation has been provided by Wittrick (1966), its solution is elaborated in that reference either for the limiting case of zero helix angle or under assumptions referred to as Bernoulli–Euler model. The danger of these assumptions has been recognized in the concluding section of the paper by Wittrick (1966), but no quantification has been provided. More detailed study of the location of dispersion curves is presented by Lee & Thompson (2001). Unfortunately, that study has not been extended to the sufficiently high-frequency region, in which the Timoshenko-type theory should actually be used. The dispersion diagrams reported by Guido *et al.* (1978) are obtained under several restricting assumptions, in particular that longitudinal inertia is negligible, which dramatically narrows their applicability. Treyssède (2008) presented detailed dispersion diagrams extended to high frequencies for helical waveguides with large pitch, which does not correspond to conventional parameters of elastic springs used in suspension systems.

The findings presented in the remaining part of this paper have been partly reported by the author at the *Int. Conf. on Sound and Vibration* (Sorokin 2008*a*) and at the *Int. Congress on Applied and Theoretical Mechanics* (Sorokin 2008*b*).

2. Alternative theories and their validity ranges

Although several theories of dynamics of helical springs can be found in the literature, only three of them can actually qualify to describe the propagation of all waves existing in such a structure, specifically dominantly longitudinal, torsion and flexural waves. These three theories employ the standard concept of plane cross sections that reduces a three-dimensional spring to the one-dimensional model of a spatial rod exposed to axial, torsion and flexural deformations.

The most general theory, which takes into account shear deformation and rotary inertia and should therefore be called the Timoshenko-type theory, is formulated by Wittrick (1966) and used in many subsequent papers. Its detailed derivation is available in these references and not repeated here. In dimensional form, the equations of dynamics of a helical spring of a radius R with the circular cross section of a coil of diameter d ($A=\pi d^2/4$, $I_p=2I_x=2I_y=\pi d^4/32$) and the pitch h are the following (figure 1):

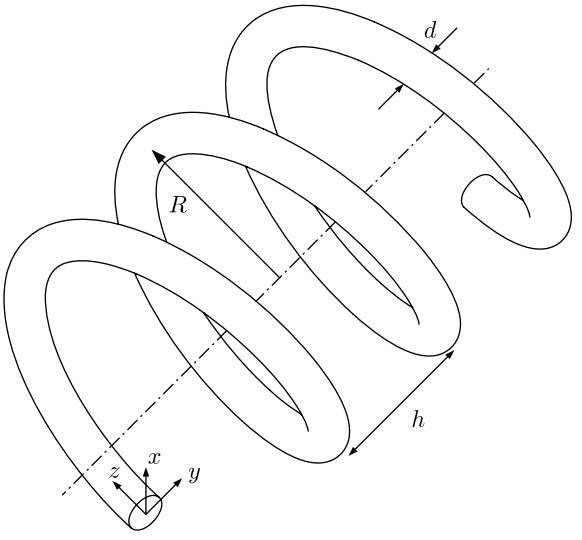

Figure 1. A helical spring: notations.

$$\rho A\frac{\partial^2\bar{u}}{\partial t^2}=\frac{\partial Q_x}{\partial\bar{s}}+\frac{\cos^2\psi}{R}N_z-\frac{\sin\psi\cos\psi}{R}Q_y, \tag{2.1a}$$

$$\rho A\frac{\partial^2\bar{v}}{\partial t^2}=\frac{\partial Q_y}{\partial\bar{s}}+\frac{\sin\psi\cos\psi}{R}Q_x, \tag{2.1b}$$

$$\rho A\frac{\partial^2\bar{w}}{\partial t^2}=\frac{\partial N_z}{\partial\bar{s}}-\frac{\cos^2\psi}{R}Q_x, \tag{2.1c}$$

$$\rho I_x\frac{\partial^2\alpha}{\partial t^2}=\frac{\partial M_x}{\partial\bar{s}}+\frac{\cos^2\psi}{R}T_z-\frac{\sin\psi\cos\psi}{R}M_y-Q_y, \tag{2.1d}$$

$$\rho I_y\frac{\partial^2\beta}{\partial t^2}=\frac{\partial M_y}{\partial\bar{s}}+\frac{\sin\psi\cos\psi}{R}M_x+Q_x, \tag{2.1e}$$

$$\rho I_p\frac{\partial^2\gamma}{\partial t^2}=\frac{\partial T_z}{\partial\bar{s}}-\frac{\cos^2\psi}{R}M_x, \tag{2.1f}$$

$$\frac{M_x}{EI_x}=\frac{\partial\alpha}{\partial\bar{s}}+\frac{\cos^2\psi}{R}\gamma-\frac{\sin\psi\cos\psi}{R}\beta, \tag{2.1g}$$

$$\frac{M_y}{EI_y}=\frac{\partial\beta}{\partial\bar{s}}+\frac{\sin\psi\cos\psi}{R}\alpha, \tag{2.1h}$$

$$\frac{T_z}{GI_p}=\frac{\partial\gamma}{\partial\bar{s}}-\frac{\cos^2\psi}{R}\alpha, \tag{2.1i}$$

$$\frac{Q_x}{\kappa GA}=\frac{\partial\bar{u}}{\partial\bar{s}}-\frac{\sin\psi\cos\psi}{R}\bar{v}+\frac{\cos^2\psi}{R}\bar{w}-\beta, \tag{2.1j}$$

$$\frac{Q_y}{\kappa GA}=\frac{\partial\bar{v}}{\partial\bar{s}}+\frac{\sin\psi\cos\psi}{R}\bar{u}+\alpha, \tag{2.1k}$$

$$\frac{N_z}{EA} = \frac{\partial \bar{w}}{\partial \bar{s}} - \frac{\cos^2\psi}{R}\,\bar{u}. \tag{2.1l}$$

In these equations, ψ is the pitch angle ($\tan\psi = h/2\pi R$), κ is the shear coefficient, E is Young's modulus, G is the shear modulus and ρ is the mass density of the spring. The coordinate $\bar{s}$ is counted along the axis of a spring, and the components of displacements (u, v, w), angles (α, β, γ), moment resultants (M_x, M_y, T_z) and force resultants (Q_x, Q_y, N_z) are directed along the axes (x, y, z) shown in figure 1.

When the pitch and the radius of curvature are set to zero, conventional theories of propagation of axial and torsion waves in a straight rod are recovered from equations (2.1*f*), (2.1*i*) and (2.1*c*), (2.1*l*), respectively. The equations of Timoshenko beam theory for flexural waves in planes XOZ and YOZ are readily recovered from the sets of equations (2.1*a*), (2.1*e*), (2.1*h*), (2.1*j*) and (2.1*b*), (2.1*d*), (2.1*g*), (2.1*k*).

Equations (2.1*a*)–(2.1*l*) are significantly simplified by neglecting the deformation due to shear and axial loads and the rotational inertias of the cross section, as shown by Pearson & Wittrick (1986). This version of the theory is referred to in that reference as an 'exact Bernoulli–Euler model'. Physically, this model ignores the dominantly axial waves and the dominantly shear waves in a helical spring. In view of the subsequent discussion in this section, it is more prudent to call it the 'simplified' or 'standard' Bernoulli–Euler model.

As is well known, the elementary theory of straight rods allows the propagation of axial, torsion and flexural waves being totally uncoupled from each other. In a helix, these waves are coupled and, therefore, the possibility to neglect the axial wave is questionable. In this paper, the theory, which follows from equations (2.1*a*)–(2.1*l*) with only rotary inertia and shear forces being neglected, is called a refined Bernoulli–Euler model.

Straightforward but cumbersome transformations yield six coupled differential equations with respect to the three displacements (u, v, w) and the three angles of rotation (α, β, γ) in the framework of the Timoshenko theory. In the case of the refined Bernoulli–Euler model, the system of governing equations contains four coupled differential equations with respect to the three displacements (u, v, w) and the torsion angle γ. In the case of the simplified Bernoulli–Euler model, the dynamics of a helical spring is described by three coupled differential equations with respect to the transverse displacements (u, v) and the torsion angle γ.

Naturally, the equations of the Timoshenko-type theory are more general than the two other sets, and they should be used as a reference to assess the validity of the simplified equations of the standard Bernoulli–Euler theory and of the refined Bernoulli–Euler theory. This assessment is a straightforward task accomplished by comparison of the location of dispersion curves predicted by these three theories. Each of these theories yields a characteristic equation of the 12th order in the wavenumber k_{dim} as soon as the standard dependence of all functions (u, v, w, α, β, γ) upon spatial and temporal coordinates $\exp(k_{\mathrm{dim}}\bar{s} - \mathrm{i}\omega t)$ is adopted (e.g. $u = U\exp(k_{\mathrm{dim}}\bar{s} - \mathrm{i}\omega t)$). The difference between the three theories manifests itself in the difference of the order of the characteristic equation in the frequency ω and in the presence of shear force effects in the Timoshenko theory. Specifically, the Timoshenko theory yields a characteristic equation of the 12th order in frequency. In the refined Bernoulli–Euler theory, this equation is of the 8th order in ω and in the simplified Bernoulli–Euler theory, the order in ω is reduced to 6.

To describe wave motion in a helical spring, it is convenient to introduce a few non-dimensional parameters. Specifically, the material of a spring is characterized by its Poisson ratio ν and its geometry is characterized by the pitch angle ψ and the diameter-to-radius ratio d/R. In the Timoshenko-type theory, a shear coefficient κ is also specified. The non-dimensional frequency parameter is introduced as $\Omega=\omega d/c$, with $c=\sqrt{E/\rho}$ as the speed of a plane dilatation wave in the material of the spring, and the non-dimensional wavenumber is $k=k_{\dim}d$. The pitch has to satisfy $h>d$ in order to ensure the absence of contact of laps of the spring.

Equations (2.1a)–(2.1l) contain the non-dimensional parameters d/R, $\cos^2\psi$ and $\sin\psi\cos\psi$. To simplify the algebra, it is convenient to introduce the small parameter $\varepsilon=d/R$ and two parameters in the following form: $q=\cos^2\psi$, $r=\sin\psi\cos\psi$. They are linked as $r^2=q(1-q)$. The parameter q is not small ($q\sim O(1)$), because the pitch angle in any suspension helical spring cannot be close to $\pi/2$. By contrast, the parameter r is small, because the pitch angle is small. Thus, the problem formulation contains two small parameters, and it is possible to perform an asymptotic analysis of the various regimes of the wave propagation. However, as a starting point, it is expedient to advance with the direct numerical resolution.

The dispersion equation in the case of the Timoshenko theory is obtained by taking the determinant of six algebraic equations with respect to the scaled amplitudes of displacements U, V, W and the rotation angles A, B, Γ to be set to zero. These equations have the following form:

$$\left.\begin{aligned}
&\left(\Omega^2-\varepsilon^2q^2+\frac{\kappa(k^2-\varepsilon^2r^2)}{2(1+\nu)}\right)U-\frac{\kappa\varepsilon kr}{1+\nu}V+\left(\varepsilon kq+\frac{\varepsilon\kappa kq}{2(1+\nu)}\right)W-\frac{\varepsilon^2\kappa r}{2(1+\nu)}\mathrm{A}\\
&\qquad-\frac{\varepsilon\kappa k}{2(1+\nu)}\mathrm{B}=0,\\
&\frac{\kappa\varepsilon kr}{1+\nu}U+\left(\Omega^2+\frac{\kappa(k^2-\varepsilon^2r^2)}{2(1+\nu)}\right)V+\frac{\varepsilon^2\kappa qr}{2(1+\nu)}W+\frac{\varepsilon\kappa k}{2(1+\nu)}\mathrm{A}-\frac{\varepsilon^2\kappa r}{2(1+\nu)}\mathrm{B}=0,\\
&-\left(\varepsilon kq+\frac{\varepsilon\kappa kq}{2(1+\nu)}\right)U+\frac{\varepsilon^2\kappa qr}{2(1+\nu)}V+\left(\Omega^2+k^2-\frac{\kappa\varepsilon^2q^2}{2(1+\nu)}\right)W+\frac{\varepsilon^2\kappa q}{2(1+\nu)}\mathrm{B}=0,\\
&-\kappa\varepsilon rU-\kappa kV+\frac{1}{8}\varepsilon[-8\kappa+(1+\nu)\Omega^2-\varepsilon^2q^2+(1+\nu)(k^2-\varepsilon^2r^2)]\mathrm{A}-\frac{(1+\nu)}{4}\varepsilon^2kr\mathrm{B}\\
&\qquad+\frac{1}{8}\varepsilon(2+\nu)\varepsilon kq\Gamma=0,\\
&\kappa kU-\varepsilon\kappa rV+\varepsilon\kappa qW+\frac{(1+\nu)}{4}\varepsilon^2kr\mathrm{A}+\frac{1}{8}\varepsilon[-8\kappa+(1+\nu)\Omega^2+(1+\nu)(k^2-\varepsilon^2r^2)]\mathrm{B}\\
&\qquad+\frac{1}{8}(1+\nu)\varepsilon^3qr\Gamma=0,\\
&-(2+\nu)\varepsilon kq\mathrm{A}+(1+\nu)\varepsilon^2qr\mathrm{B}+[k^2+2(1+\nu)\Omega^2-(1+\nu)\varepsilon^2q^2]\Gamma=0.
\end{aligned}\right\}\tag{2.2}$$

In the case of the refined Bernoulli–Euler theory, the determinant of four algebraic equations with respect to the scaled displacements U, V, W and the rotation angle Γ is set to zero,

$$\left.\begin{aligned}
&\left(-k^4+16\Omega^2-16\varepsilon^2q^2+6\varepsilon^2k^2r^2-\frac{\varepsilon^4q^2r^2}{1+\nu}-\varepsilon^4r^4\right)U\\
&\quad+\left(4\varepsilon k^3r-\frac{\varepsilon^3kq^2r}{1+\nu}-4\varepsilon^3kr^3\right)V+(16\varepsilon kq-\varepsilon k^3q+3\varepsilon^3kqr^2)\,W\\
&\quad-\left(2\varepsilon^2kqr+\frac{\varepsilon^2kqr}{1+\nu}\right)\Gamma=0,\\
&-\left(4\varepsilon k^3r-\frac{\varepsilon^3kq^2r}{1+\nu}-4\varepsilon^3kr^3\right)U+\left(-k^4+16\Omega^2+\frac{\varepsilon^2q^2k^2}{1+\nu}+6\varepsilon^2k^2r^2-\varepsilon^4r^4\right)V\\
&\quad+(-3\varepsilon^2k^2qr+\varepsilon^4qr^3)\,W+\left(\varepsilon k^2q+\frac{\varepsilon k^2q}{1+\nu}-\varepsilon^3qr^2\right)\Gamma=0,\\
&\quad-(16\varepsilon kq-\varepsilon k^3q+3\varepsilon^3kqr^2)\,U+(-3\varepsilon^2k^2qr+\varepsilon^4qr^3)\,V\\
&\quad+(16k^2+16\Omega^2+\varepsilon^2k^2q^2-\varepsilon^4q^2r^2)\,W+\varepsilon^3q^2r\Gamma=0,\\
&\left(2\varepsilon^2kqr+\frac{\varepsilon^2kqr}{1+\nu}\right)U+\left(\varepsilon k^2q+\frac{\varepsilon k^2q}{1+\nu}-\varepsilon^3qr^2\right)V+\varepsilon^3q^2rW\\
&\quad+\left(\frac{k^2}{1+\nu}+2\Omega^2-\varepsilon^2q^2\right)\Gamma=0.
\end{aligned}\right\}\tag{2.3}$$

In the case of the simplified Bernoulli–Euler theory, the determinant of three algebraic equations with respect to the scaled displacements U, V and the rotation angle Γ is set to zero,

$$\left.\begin{aligned}
&[-(1+\nu)k^4+(6\varepsilon^2r^2(1+\nu)+\varepsilon^2q^2)k^2-(1+\nu)\varepsilon^4r^4+16(1+\nu)\Omega^2]\,V\\
&\quad+\left[-4(1+\nu)\frac{r}{q}k^4+\left(4\varepsilon^2\frac{r^3}{q}(1+\nu)-(2+3\nu)\varepsilon^2rq\right)k^2-(1+\nu)\varepsilon^4r^3q\right]W\\
&\quad+[(2+\nu)\varepsilon qk^2-(1+\nu)\varepsilon^3qr^2]\Gamma=0,\\
&\left[-4(1+\nu)\frac{r}{q}k^4+\left(4\varepsilon^2\frac{r^3}{q}(1+\nu)-(2+3\nu)\varepsilon^2rq\right)k^2-(1+\nu)\varepsilon^4r^3q\right]V\\
&\quad+\left[\frac{(1+\nu)}{\varepsilon^2q^2}k^6-(1+\nu)\left(2-6\varepsilon^2\frac{r^2}{q^2}\right)k^4+\left((1+\nu)\left(\frac{r^4}{q^2}-6+q^2\right)+r^2\right)\varepsilon^2k^2\right.\\
&\quad\left.-(1+\nu)\varepsilon^4r^2q^2+16(1+\nu)\Omega^2\right]W+[(3+2\nu)\varepsilon rk^2-(1+\nu)\varepsilon^3qr^2]\Gamma=0,\\
&[(2+\nu)\varepsilon qk^2-(1+\nu)\varepsilon^3qr^2]\,V+[(3+2\nu)\varepsilon rk^2-(1+\nu)\varepsilon^3qr^2]\,W\\
&\quad+[k^2-(1+\nu)\varepsilon^2q^2+2(1+\nu)\Omega^2]\Gamma=0.
\end{aligned}\right\}\tag{2.4}$$

The corresponding dispersion equations are readily available in a closed analytical form, but they are too cumbersome to be presented here. It is a trivial task to solve the characteristic equation for each frequency by means of standard

polynomial solvers, provided that all the parameters of the helix are given. Prior to a selection of representative geometry parameters for the comparison of the different theories, it is helpful to estimate the meaningful frequency ranges.

As is well known from the theory of wave propagation in straight rods, the elementary modelling of flexural waves based on the plane cross-section hypothesis in the framework of the Timoshenko theory is valid up to the cut-on frequency of the dominantly shear wave. This phenomenon occurs at $\Omega \approx 2$, and this is a very high frequency indeed. For a massive steel wire of diameter $d=12$ mm (see Lee & Thompson 2001), it is $f \approx 135$ kHz. For a steel wire of diameter $d=1$ mm (see Lee 2007), it is $f \approx 1.6$ MHz. The classical Bernoulli–Euler theory fails to describe the propagation of a flexural wave in a straight rod approximately at $\Omega \approx 0.25$. Therefore, it is practical to take $\Omega \approx 0.25$ as the upper limit of the frequency range, where it is meaningful to compare the three theories. For steel wires of diameter $d=1$ and 12 mm, it is still a very high frequency: $f \approx 160$ kHz (the highest eigenfrequency reported by Lee (2007) is approx. 1 kHz) and $f \approx 13.5$ kHz (the highest eigenfrequency reported by Lee & Thompson (2001) is approx. 100 Hz), respectively. Although the problem of the calculation of the eigenfrequencies is deliberately left out of the scope of this paper, it is appropriate to mention that the validity of the dispersion equations (2.2) and (2.3) has been checked by comparing the eigenfrequencies obtained by the boundary integral equation method with the results reported by Mottershead (1980), Lee & Thompson (2001) and Lee (2007). It is reasonable to expect that within the range $0<\Omega<0.25$, 'high' frequencies should be distinguished from 'low' frequencies. This heuristic statement is validated in §3 by means of a classical asymptotic analysis, but for the purpose of comparison of the three theories, an 'ad hoc' criterion may be introduced. The low-frequency range is defined as $0 \leq \Omega \leq 0.025$ and a high-frequency range is defined as $0.025 \leq \Omega \leq 0.25$.

Consider a 'thick' spring with $d/R=0.184$ and $\psi=0.13$. This set of parameters has been used by Lee & Thompson (2001). The dispersion curves are presented in figure 2 in the low-frequency region. Owing to the natural symmetry of the considered waveguide, if k satisfies the dispersion equation, then $-k$ is also its root, and it is thus sufficient to compare the location of dispersion curves with Re $k \geq 0$ and Im $k \geq 0$. Purely real wavenumbers (in notations used in this paper, they represent non-propagating waves) and real parts of complex-valued wavenumbers are shown in figure 2*a*. Purely imaginary wavenumbers (i.e. those of propagating waves) and imaginary parts of complex-valued wavenumbers are shown in figure 2*b*. For definiteness, in the following, the shear coefficient of the Timoshenko theory for a circular cross section is chosen as recommended, for example by Shames & Dym (1991), as $\kappa = (6(1+\nu))/(7+6\nu)$ (the ambiguity in selection of the value of this coefficient does not undermine the asymptotic results reported in §3). At this stage of analysis, the interest is focused on the validity ranges of the three theories and, therefore, the same symbols are used to designate all wavenumbers within the same theory. For studying fine details in dispersion diagrams in §3 of this paper, three types of wavenumbers will certainly be distinguished. Alongside this, the identification of eigenmodes associated with each branch is postponed to §§3 and 4. Results reported in the remaining part of this section should be regarded in the first instance as an output of numerical experiments, which has to be explained theoretically, as is done in §3.

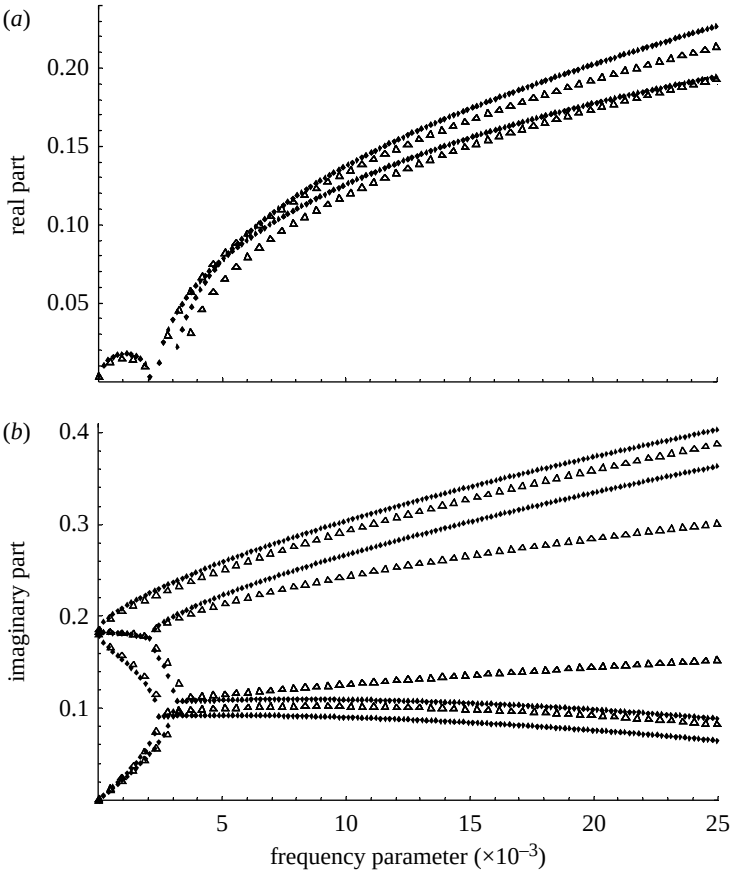

Figure 2. Comparison of dispersion curves in the low-frequency range for a 'thick' spring, $d/R=0.184$ and $\psi=0.13$. (*a*) Real and (*b*) imaginary parts of wavenumbers. Dotted lines, the Timoshenko theory; triangles, the standard Bernoulli–Euler theory.

In the frequency range shown in figure 2, the Timoshenko theory and the refined Bernoulli–Euler theory yield undistinguishable dispersion curves, whereas, as clearly seen, the standard Bernoulli–Euler theory has a limited validity range and it fails at approximately $\Omega\approx0.003$. Corrections introduced by the Timoshenko model become significant only at $\Omega\approx0.1$, as seen from figure 3. The Timoshenko theory and the refined Bernoulli–Euler theory disagree only about the location of two sets of dispersion curves for large wavenumbers at sufficiently high frequencies. As may be intuitively guessed and as is proved in §3, these branches present wavenumbers of dominantly flexural waves.

For a thick spring with a large pitch angle, $d/R=0.184$ and $\psi=\pi/6$, the standard Bernoulli–Euler theory fails at low frequencies, already at $\Omega\approx0.001$. This is obvious from figure 4, where notations and frequency range are the same as in figure 2, and it leads to the conclusion that this theory does not qualify to be used in the analysis of vibrations of flexible springs. The refined Bernoulli–Euler model is applicable in the same frequency range as in the case of a thick spring with a small pitch. This is seen in figure 5, where the same designation of curves

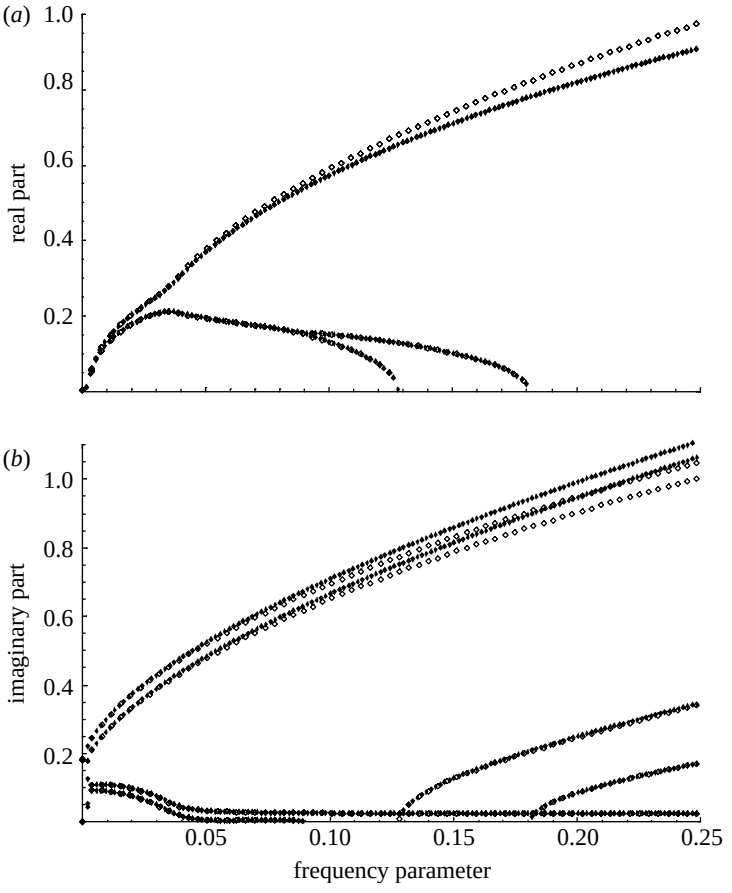

Figure 3. Comparison of dispersion curves in the high-frequency range for a 'thick' spring, $d/R=0.184$ and $\psi=0.13$. (*a*) Real and (*b*) imaginary parts of wavenumbers. Dotted lines, the Timoshenko theory; rhombus symbols, the refined Bernoulli–Euler theory.

and the same frequency range as in figure 3 are employed. As a spring becomes thinner, the validity range of the standard Bernoulli–Euler theory shrinks virtually to zero.

These results of direct numerical resolution of the dispersion equations have an obvious physical explanation. The refined Bernoulli–Euler model correctly describes axial and torsion waves and the Timoshenko model does not contribute any significant corrections to this description. In other words, axial and torsion waves are weakly coupled with flexural waves in the high-frequency range, whereas, in the low-frequency range, the Timoshenko corrections are asymptotically small. Flexural waves in a helical spring are influenced by rotary inertia and shear forces, roughly speaking, to the same extent as in the straight rod. Therefore, the refined Bernoulli–Euler model for a helix fails virtually at the same frequency as for a straight beam. This failure manifests itself only in an improper description of flexural waves at high frequencies.

The standard Bernoulli–Euler model appears to be incorrect at low frequencies because the interaction between axial and flexural waves is particularly important there. This interaction becomes more pronounced as

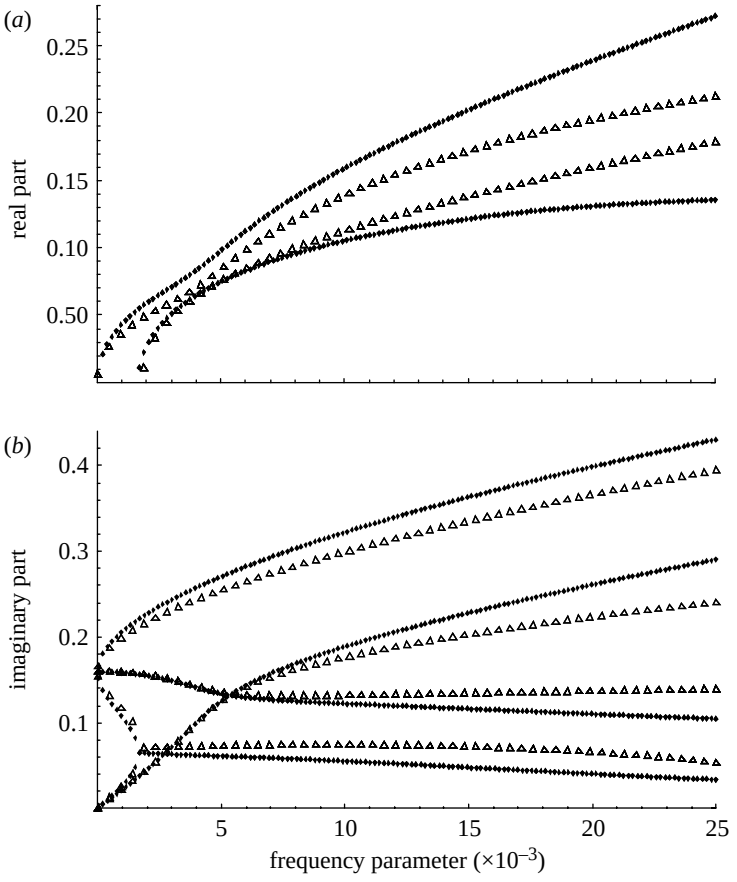

Figure 4. Comparison of dispersion curves in the low-frequency range for a 'thick' spring with a large pitch angle, $d/R=0.184$ and $\psi=\pi/6$. (*a*) Real and (*b*) imaginary parts of wavenumbers. Symbols are same as defined in legend of figure 2.

the pitch angle increases. At high frequencies, this theory should be disqualified because it does not capture the dominantly axial wave. It should be pointed out that the role of in-plane inertia in the vibrations of curved planar beams has been discussed in numerous publications (e.g. the survey by Chidamparam & Leissa 1993).

On balance, it is obvious that the problem in the analysis of wave motion in helical springs is readily solved numerically within the framework of refined Bernoulli–Euler model when, roughly speaking, $\Omega<0.1$. The Timoshenko theory should be applied when $\Omega>0.1$. The reported results suggest that the assumption employed, for example, by Wittrick (1966, §§7 and 8), which leads from the refined Bernoulli–Euler theory to its standard version, is dangerous because it erroneously predicts the location of the whole set of dispersion curves even at low frequencies. However, such a simple qualification does not yield an insight into specific features of wave motion related to each branch in the dispersion diagram and into the role of parameters involved in the problem formulation.

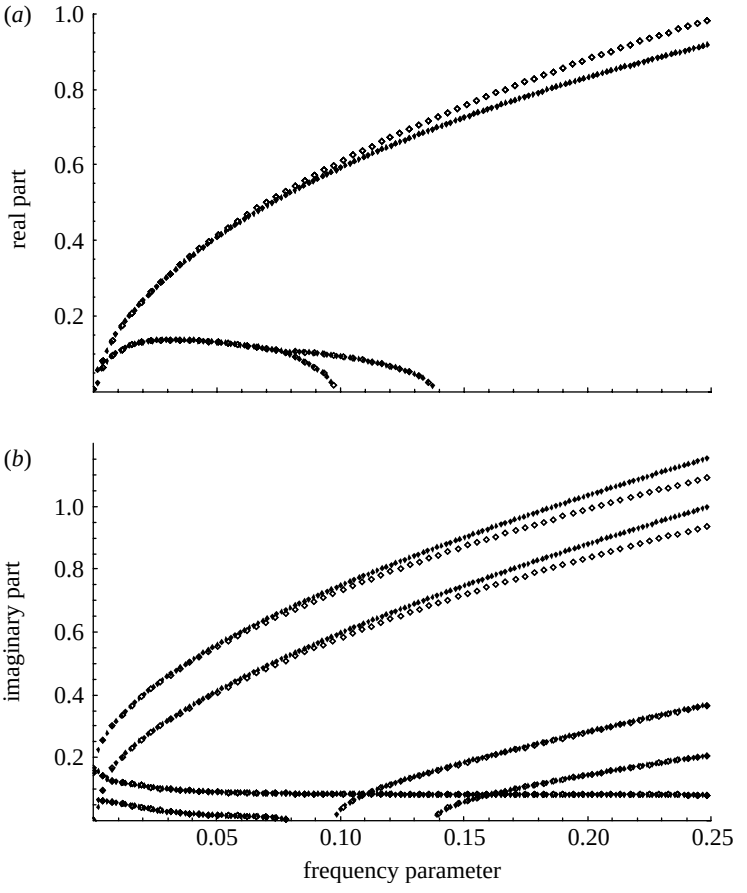

Figure 5. Comparison of dispersion curves in the high-frequency range for a 'thick' spring with a large pitch angle, $d/R=0.184$ and $\psi=\pi/6$. (*a*) Real and (*b*) imaginary parts of wavenumbers. Symbols are same as defined in legend of figure 3.

3. Regimes of wave motion and asymptotic formulae for wave numbers

As is discussed in §2, at least two distinct frequency ranges may be identified in the analysis of wave motion in helical springs. This ad hoc statement can be rigorously proved by means of a classical asymptotic analysis of the governing equations. Inasmuch as the simplified Bernoulli–Euler theory is shown to be not satisfactorily accurate, this section is concerned with an asymptotic analysis of its refined counterpart and, as much as it is necessary, of the Timoshenko theory.

Equations (2.2) and (2.3) contain two small parameters $\varepsilon=d/R$ and $r=\sin\psi\cos\psi$. The dispersion equation in each case also includes the wavenumber k and the frequency parameter Ω. Apparently, the 'principal' small parameter in the problem formulation is ε. Then, following, for example, Hinch (1991), all other parameters involved in the problem formulation should be expressed in powers of this parameter, namely

$$r = r_0\varepsilon^p, \tag{3.1a}$$

$$\Omega = \Omega_0\varepsilon^j, \tag{3.1b}$$

$$k = K_0\varepsilon^n + K_1\varepsilon^m + \cdots, \tag{3.1c}$$

where $r_0 \sim O(1)$, $\Omega_0 \sim O(1)$, $K_0 \sim O(1)$, $K_1 \sim O(1)$ and $m > n$.

Substitution of formulae (3.1*a*)–(3.1*c*) into the dispersion equations, which follow from (2.2) and (2.3), presents all their terms expressed in various powers of the small parameter ε, and the dominant balance is achieved when the maximum number of terms is of the same leading order. Such an analysis is not feasible unless a symbolic manipulator, e.g. MATHEMATICA (Wolfram 1991), is used.

It is also helpful to observe the heuristic discussion of the frequency ranges of practical interest reported in §2. The low-frequency regime may be defined by setting $j=2$ and the high-frequency range is related to $j=1$. Another useful observation is related to the fact that, in a straight beam, there coexist longitudinal and torsion waves, for each of which $n=j$, and flexural waves, for each of which $n=(1/2)j$.

(*a*) *High-frequency asymptotic expansions*

In the high-frequency limit, $p=1/2$, $j=1$ and two significant regimes are identified. The first one describes dominantly flexural waves: $n=1/2$ and $m=3/2$. The second one is applicable for the waves of in-plane (axial) and anti-plane (torsion) deformation: $n=1$ and $m=3$.

In the former case, the non-dimensional wavenumbers are multiple to the leading order and they correspond to conventional propagating and evanescent flexural waves in two orthogonal planes in a straight rod. They are split into two branches each due to the Poisson effect and spatial progress of helix. Explicit formulae in the original variables are compact:

Propagating flexural waves,

$$k_{1,2,3,4} = \pm\frac{\mathrm{i}}{16\Omega^{1/2}}\left[32\Omega + (6+\nu)\varepsilon^2 q^2 \pm \sqrt{\nu^2\varepsilon^2 q^4 + 256\varepsilon^2 r^2\Omega}\right], \tag{3.2a}$$

evanescent flexural waves,

$$k_{5,6,7,8} = \pm\frac{1}{16\Omega^{1/2}}\left[32\Omega - (6+\nu)\varepsilon^2 q^2 \pm \sqrt{\nu^2\varepsilon^2 q^4 - 256\varepsilon^2 r^2\Omega}\right]. \tag{3.2b}$$

The torsion wave is defined as

$$k_{9,10} = \pm\frac{\sqrt{1+\nu}}{32}\left[32\sqrt{\varepsilon^2 q^2 - 2\Omega^2} + \frac{(2+\nu)^2\varepsilon^2 q^2}{\Omega^2}(\varepsilon^2 q^2 - 2\Omega^2)^{3/2}\right]. \tag{3.2c}$$

The longitudinal wave is defined as

$$k_{11,12} = \pm\frac{\sqrt{\varepsilon^2 q^2 - \Omega^2}}{8\Omega^2}[\varepsilon^4 q^4 + (8 - \varepsilon^2 q^2)\Omega^2]. \tag{3.2d}$$

Naturally, these formulae merge into their counterparts for a straight rod if one sets $\varepsilon = r = 0$. It is worth noting that, in this regime, the torsion wave and longitudinal wave are influenced by the curvature of the helix, but this influence is controlled by the 'in-plane' curvature q, rather than by the 'out-of-plane'

curvature r. In other words, these two waves do not 'distinguish' a helix from a ring, up to the second-order terms. By contrast, flexural waves are strongly influenced by the curvature of a helix both in plane and out of plane.

Formulae (3.2c) and (3.2d) for $\Omega \gg \varepsilon q$ yield standard dispersion relations for shear and dilatation waves: $k = \pm \mathrm{i}\Omega\sqrt{2(1+\nu)}$ and $k = \pm \mathrm{i}\Omega$. However, these asymptotic formulae predict a crossing of branches of dispersion curves, which occurs below the cut-on frequency of the torsion wave, i.e. within a relatively low-frequency range. Inasmuch as eigenmodes associated with these wavenumbers are not orthogonal, formulae (3.2c) and (3.2d) become invalid in this zone of the (k, Ω) space. This issue is discussed in the context of the analysis of the validity of asymptotic formulae in §3d.

In §2, it has been shown that the difference between the refined Bernoulli–Euler model and the Timoshenko model manifests itself only in the high-frequency range in the description of dominantly flexural waves. This statement is fully confirmed by applying the reported high-frequency scaling to dispersion equations. Up to the first-order correction, formulae (3.2c) and (3.2d) are valid for the description of dominantly longitudinal and dominantly torsion waves. However, formulae (3.2a) and (3.2b) for dominantly flexural waves should be revised in the framework of the Timoshenko theory. Specifically, they acquire the following form:

propagating waves,

$$k_{1,2,3,4} = \pm \frac{\mathrm{i}}{16\Omega^{1/2}} \left[\left(2 + \frac{4(1+\nu)}{\kappa} \right) \Omega^2 + 32\Omega + (6+\nu)\varepsilon^2 q^2 \pm \sqrt{\nu^2 \varepsilon^2 q^4 + 256 \varepsilon^2 r^2 \Omega} \right], \tag{3.3a}$$

evanescent waves,

$$k_{5,6,7,8} = \pm \frac{1}{16\Omega^{1/2}} \left[-\left(2 + \frac{4(1+\nu)}{\kappa} \right) \Omega^2 + 32\Omega - (6+\nu)\varepsilon^2 q^2 \pm \sqrt{\nu^2 \varepsilon^2 q^4 - 256 \varepsilon^2 r^2 \Omega} \right]. \tag{3.3b}$$

Naturally, the corrections in comparison with formulae (3.2a) and (3.2b) are of order 3/2 in Ω and they merge standard formulae for wavenumbers in the Timoshenko theory of straight beams when $\varepsilon \to 0$.

It should be pointed out that the high-frequency regime might rather be called the mid-frequency one, inasmuch as the asymptotic formulae (3.3a) and (3.3b) are not valid for large magnitudes of the frequency parameter $\Omega \equiv \omega d/c$, say, for $\Omega > 2$. However, a detailed inspection into this regime of wave motion is not practical, because the theory of helical springs (even in the Timoshenko-type formulation) implies certain kinematic hypotheses concerning the deformation of cross sections of a rod. These hypotheses do not hold at high frequencies and the three-dimensional theory of elasticity should be used for the analysis of wave motion in this case (see Treyssède 2008).

(*b*) *Low-frequency asymptotic expansions*

In the low-frequency regime, the dominant balance is reached with the following scaling: $j = 2$, $p = 0$, $n = 1$ and $m = 3$. As is seen already from this scaling,

the contribution of flexural deformation is essential for all waves. To the leading order, the dispersion equation reads as (at $p=0$, $r\equiv r_0$)

$$K_0^{12}+4qK_0^{10}+\left[-32\Omega_0^2+6q^2\right]K_0^8+4\left[q^3+4\Omega_0^2(-(2-\nu)q^2+12r^2)\right]K_0^6 +\left[256\Omega_0^4+q^4+32\Omega_0^2((1+\nu)q^4-3\nu q^2r^2-r^4)\right]K_0^4 -16(2+\nu)\Omega_0^2q^2\left(16\Omega_0^2-q^2\right)K_0^2+256(1+\nu)\Omega_0^4q^4=0. \tag{3.4}$$

It does not present any difficulties to solve this equation in MATHEMATICA (Wolfram 1991), but the final answer in an explicit analytical form is not available. A failure to reduce the order of polynomial, which determines the leading order terms in the asymptotic expansion (3.1*c*), suggests that, at low frequencies, there is a global coupling of all types of deformations in a helical spring. A detailed inspection into quasi-statics in §3*c* shows that, in contrast to this case, the explicit asymptotic formulae in the 'naive' limit $\Omega\to0$ have a narrow validity range.

The second term K_1 in the asymptotic expansion (3.1*c*) is found to be

$$\left.\begin{aligned}
K_1&=\frac{Z_1}{Z_2},\\
Z_1&=\Omega_0^2\left(z_{11}K_0^{10}+z_{12}K_0^8+z_{13}K_0^6+z_{14}K_0^4+z_{15}K_0^2+z_{16}\right),\\
z_{11}&=-(3+2\nu),\quad z_{12}=-(3+4\nu)q^2-4(3+2\nu)r^2,\\
z_{13}&=32(3+2\nu)\Omega_0^2+(3-2\nu)q^4-3(5+4\nu)q^2r^2-6(3+2\nu)r^4,\\
z_{14}&=4\nu\left[4\Omega_0^2(q^2-24r^2)-r^2(q^4+3q^2r^2+2r^4)\right]\\
&\quad+3\left[q^6-2q^4r^2-7q^2r^4-4\left(48\Omega_0^2r^2+r^6\right)\right],\\
z_{15}&=-256(3+2\nu)\Omega_0^4-r^2q^2[3q^2+(3+2\nu)r^2]+16\Omega_0^2[3(2+\nu)q^4\\
&\quad+3(1+2\nu)q^2r^2+2(3+2\nu)r^4],\\
z_{16}&=-16\Omega_0^2q^2\left[-48(1+\nu)\Omega_0^2+(3-2\nu)q^2r^2+3(1+\nu)r^4\right],\\
Z_2&=4K_0\left[3K_0^{10}+10qK_0^8+z_{23}K_0^6+z_{24}K_0^4+z_{25}K_0^2+z_{26}\right],\\
z_{23}&=4\left[-16\Omega_0^2+3q^2\right],\quad z_{24}=6\left[q^3-4(2-\nu)\Omega_0^2q^2+48\Omega_0^2r^2\right],\\
z_{25}&=256\Omega_0^4+q^4+32\Omega_0^2[(1+\nu)q^4-3\nu q^2r^2-r^4],\\
z_{26}&=-8(2+\nu)\Omega_0^2q^2\left[16\Omega_0^2-q^2\right].
\end{aligned}\right\} \tag{3.5}$$

Naturally, in the trivial case of $\psi=0$, a helix degenerates into a circular ring, $r=0$, $q=1$, and the leading order equation (3.4) readily factorizes into the product of two bi-cubic equations,

$$K_0^6 + 2K_0^4 + \left(1 - 16\Omega_0^2\right)K_0^2 + 16\Omega_0^2 = 0, \tag{3.6a}$$

$$K_0^6 + 2K_0^4 + \left(1 - 16\Omega_0^2\right)K_0^2 + 16(1+\nu)\Omega_0^2 = 0. \tag{3.6b}$$

The first one describes coupled longitudinal and in-plane flexural wave motion in a ring, while the second one describes coupled torsion and out-of-plane flexural wave motion. The first-order correction term K_1 is readily available from equation (3.5) as it is simplified by setting $r=0$, $q=1$. This limiting case has been thoroughly analysed in §6 of the paper by Wittrick (1966). By contrast, the low-frequency scaling, which yields equations (3.4) and (3.5), is valid for arbitrary pitch angles. Therefore, it is expedient to inspect the structure of eigenmodes without restricting the magnitude of a pitch angle. Besides practical relevance of its own right, such an analysis allows an assessment of the validity of results reported in the above-mentioned reference. This is accomplished in §4.

(*c*) *Quasi-statics*

Another meaningful limit case is the static deformation of a helical spring. When the frequency parameter Ω_0 is set to zero, equation (3.4) reduces to

$$\left[K_0^2 + q\right]^4 K_0^4 = 0,$$

which yields three sets of multiple roots of fourth-order each, in the variables $k=0$, $k=\mathrm{i}(d/R)\cos\psi$ and $k=-\mathrm{i}(d/R)\cos\psi$. Explicit formulae for the wavenumbers with positive imaginary parts (i.e. those with positive phase speed) are the following.

Propagating flexural waves,

$$k_{3,4} = \mathrm{i}\varepsilon\sqrt{q} \pm \mathrm{i}2^{3/4}\sqrt{\Omega}\sqrt[4]{\frac{r^2}{q}(2+\nu q)} - \mathrm{i}\sqrt{2}\,\frac{\nu\Omega \mathrm{r}}{\varepsilon}\,\frac{1}{\mathrm{q}\sqrt{2\mathrm{q}+\nu\mathrm{q}^2}}, \tag{3.7a}$$

evanescent flexural waves,

$$k_{1,2} = \mathrm{i}\varepsilon\sqrt{q} \pm 2^{3/4}\sqrt{\Omega}\sqrt[4]{\frac{r^2}{q}(2+\nu q)} + \mathrm{i}\sqrt{2}\,\frac{\nu\Omega \mathrm{r}}{\varepsilon}\,\frac{1}{\mathrm{q}\sqrt{2\mathrm{q}+\nu\mathrm{q}^2}}. \tag{3.7b}$$

The torsion wave is defined as

$$k_5 = \frac{4\mathrm{i}\Omega\sqrt{1+\nu}}{\varepsilon} + \frac{32\mathrm{i}\Omega^3}{\varepsilon^5}\,\frac{(3+2\nu)q^4 + 2(6+5\nu)q^2r^2 + r^4}{q^4}. \tag{3.7c}$$

The longitudinal wave is defined as

$$k_6 = \frac{4\mathrm{i}\Omega}{\varepsilon} + \frac{32\mathrm{i}\Omega^3}{\varepsilon^5}\,\frac{3q^4 - 4q^2r^2 + r^4}{q^4}. \tag{3.7d}$$

Obviously, the elementary models of a spring reduced to an equivalent rod are readily captured by the asymptotic formulae (3.7*c*) and (3.7*d*). Indeed, the model of propagation of a globally extensional wave is available as the first term in formula (3.7*c*). The 'macroscopic' elongation/shortening of a spring

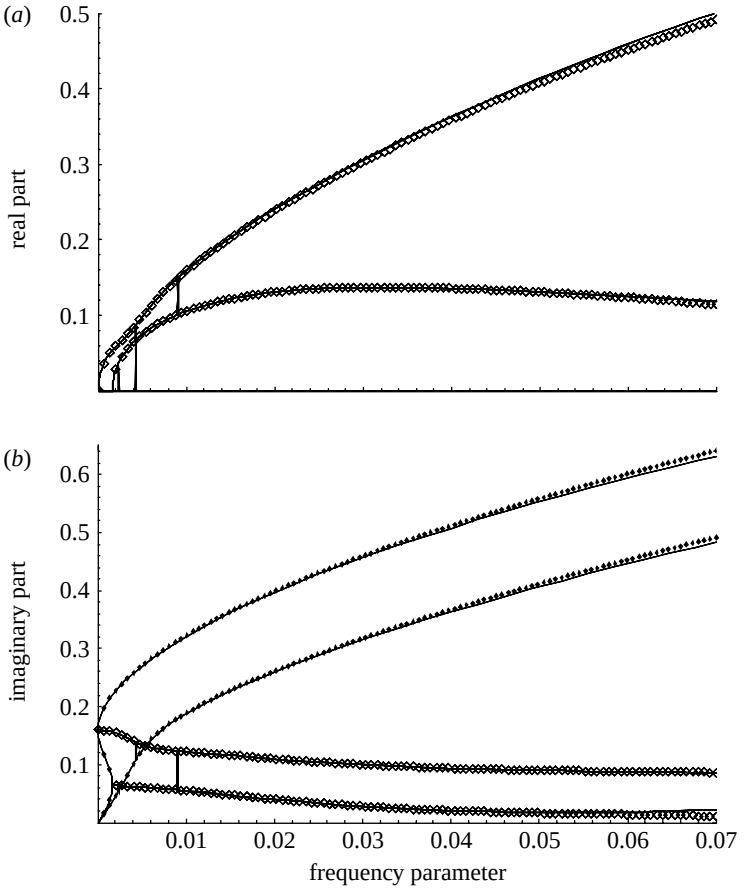

Figure 6. Low-frequency asymptotic of dispersion curves for a 'thick' spring with a large pitch angle, $d/R=0.184$ and $\psi=\pi/6$. (*a*) Real and (*b*) imaginary parts of wavenumbers. Symbols are the same as defined in legend of figure 3.

is produced by coupled torsion and flexure in a coil. Similarly, the propagation of a global rotational wave is associated with the axial deformation in a coil and it is described by the leading order term in formula (3.7*d*). Unfortunately, these primitive models have an extremely narrow range of validity, as is demonstrated in §3*d*.

(*d*) *Comparison with exact solution*

There are two tasks in reporting results of the asymptotic analysis of the dispersion relation for a helical spring. The first one is to show that both the low-frequency and high-frequency asymptotic formulae presented in §3*a*,*b* match the exact dispersion diagram for a representative set of parameters involved in the problem formulation. The second task is to inspect the location of the dispersion curves in the overlapping region.

In figures 6–10, dotted lines designate purely real and purely imaginary roots of dispersion equation obtained from the exact formulation of the dispersion equation. Rhomb symbols are used to designate real and imaginary parts of

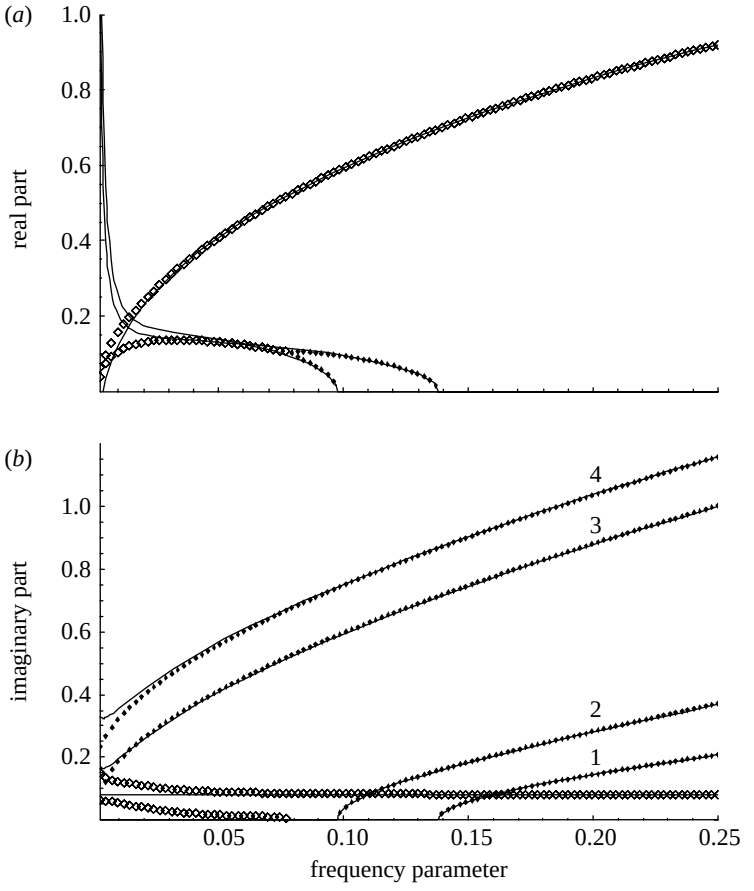

Figure 7. High-frequency asymptotic of dispersion curves for a 'thick' spring with a large pitch angle, $d/R=0.184$ and $\psi=\pi/6$. (*a*) Real and (*b*) imaginary parts of wavenumbers. Symbols are the same as defined in legend of figure 3.

complex roots. Thin continuous lines are plotted after asymptotic formulae for the low-frequency regime (3.4) and (3.5), and thick continuous lines are plotted after asymptotic formulae for the high-frequency regime (3.2*c*), (3.2*d*), (3.3*a*) and (3.3*b*).

Dispersion curves for a thick spring with a large pitch angle ($d/R=0.184$, $\psi=\pi/6$) are plotted in the low-frequency range in figure 6. In this regime, the refined Bernoulli–Euler theory gives the same results as the Timoshenko theory. Discrepancies between asymptotic predictions and exact solution can be seen only at $\Omega>0.06$. Vertical lines between curves in this figure are merely a 'by-product' of plotting dispersion curves as continuous lines in the graphical package. High-frequency asymptotic formulae are compared with exact solution for the same spring in figure 7. They agree accurately for $\Omega>0.06$. In figure 7*b*, curve 1 is plotted after formula (3.2*d*) for longitudinal propagating wave, curve 2 presents propagating torsion wave (3.2*c*) and curves 3 and 4 are plotted for propagating flexural waves after formula (3.3*a*) with the obvious choice of signs.

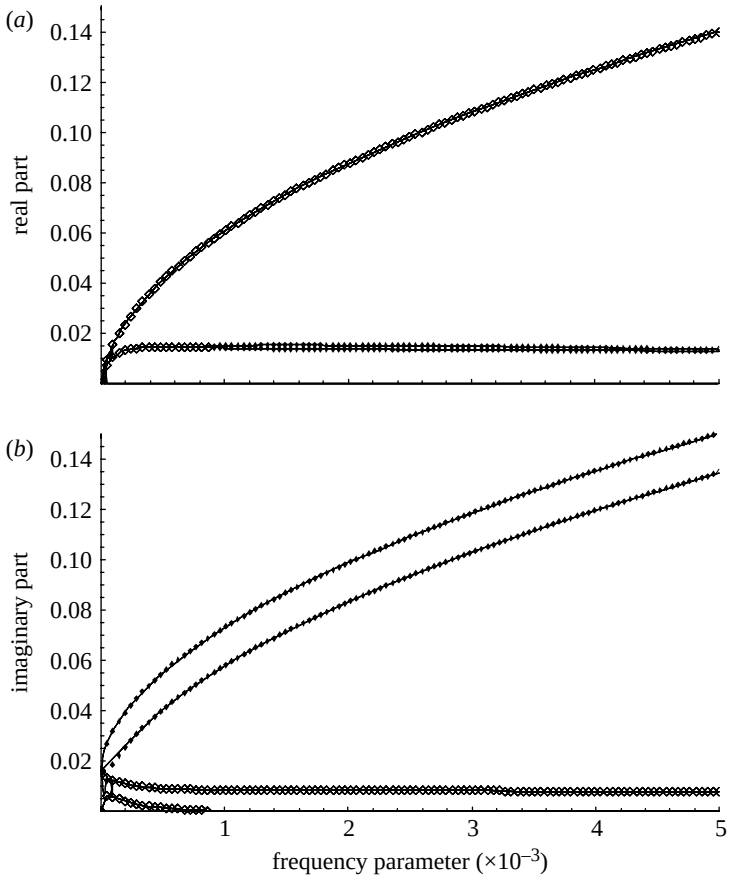

Figure 8. Low-frequency asymptotic of dispersion curves for a 'thin' spring with a large pitch angle, $d/R=0.0184$ and $\psi=\pi/6$. (*a*) Real and (*b*) imaginary parts of wavenumbers. Symbols are the same as defined in legend of figure 3.

As is seen from both figures, the 'challenging' zone in the dispersion diagram is located in the vicinity of the point where high-frequency asymptotic formulae for torsion and axial branches predict their crossing ($\Omega=0.0598$, $k=0.1256$) below their cut on.

For a 'thin' spring with the same large pitch angle ($d/R=0.184$, $\psi=\pi/6$), similar graphs are plotted in figure 8 (low-frequency regime) and figure 9 (high-frequency regime). In figure 8, it is clearly seen that a pair of complex conjugate roots is transformed into a pair of purely real roots of almost the same magnitude at the frequency $\Omega\approx0.9\times10^{-3}$, and it is accurately captured by the low-frequency asymptotic formulae. The overlapping zone between low- and high-frequency regimes is zoomed in figure 10 in the challenging zone. The low-frequency formulae accurately predict the first transformation of roots at $\Omega\approx0.9\times10^{-3}$, but they fail shortly afterwards. The high-frequency asymptotic formulae (3.2*c*) and (3.2*d*) nicely take over, but they do not adequately describe the second 'backward' splitting of two purely real wavenumbers into a pair of complex conjugate roots in the range $0.0056<\Omega<0.0062$ in a

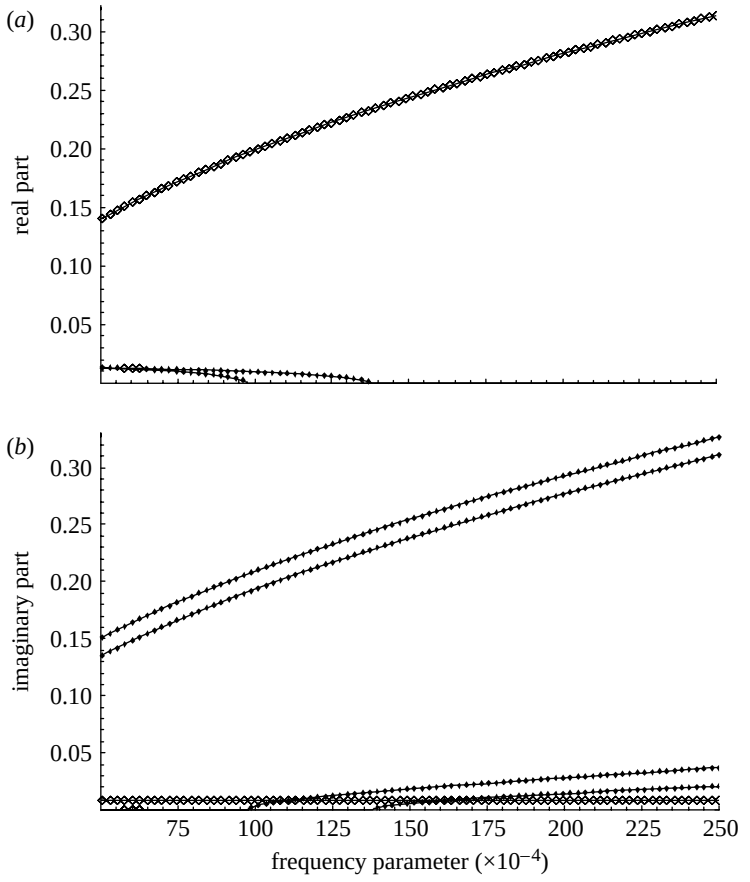

Figure 9. High-frequency asymptotic of dispersion curves for a 'thin' spring with a large pitch angle, $d/R=0.0184$ and $\psi=\pi/6$. (*a*) Real and (*b*) imaginary parts of wavenumbers. Symbols are the same as defined in legend of figure 3.

'veering' manner to avoid crossing each other—a small imaginary part of these complex roots can be seen in this range in figure 10*b*. The high-frequency asymptotic expansions for these roots recover their validity quickly and perfectly describe behaviour of dispersion curves well below cut-on frequencies and, naturally, above them. It is a fairly straightforward task to formulate a local asymptotic expansion for the roots (3.2*c*) and (3.2*d*) in the vicinity of the point in the (Ω, k) plane, where $k_9=k_{11}$ (e.g. Sorokin & Peake 2006). However, this aspect of analysis of the location of dispersion curves lies beyond the scope of the present paper, since such a description of fine details of dispersion diagrams should be done within the significant regimes (dominant balances) already established here.

Returning to the dimensional parameters employed by Lee & Thompson (2001): steel coil with $d=12$ mm, radius of helix $R=65$ mm, so that $d/R=0.184$, the threshold frequency between these two regimes ($\Omega\approx0.06$) in the case illustrated in figures 6 and 7 is approximately $f=3.6$ kHz. It is the same

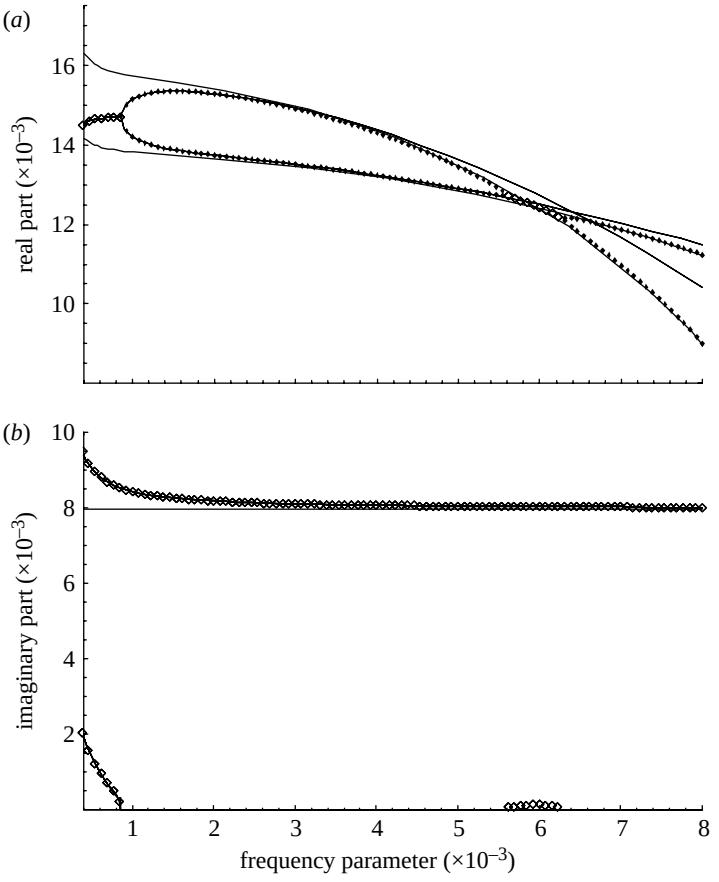

Figure 10. Overlapping region between high- and low-frequency asymptotic of dispersion curves for a 'thin' spring with a large pitch angle, $d/R=0.0184$ and $\psi=\pi/6$. (*a*) Real and (*b*) imaginary parts of wavenumbers. Symbols are the same as defined in legend of figure 3.

dimensional frequency as for the thin spring (the case illustrated in figures 8–10: steel coil with $d=1.2$ mm, radius of helix $R=65$ mm, so that $d/R=0.0184$), but in the non-dimensional form $\Omega\equiv\omega d/c$, it is $\Omega\approx 0.006$.

Finally, the low-frequency dispersion curves predicted by formulae (3.7*a*)–(3.7*d*) are shown in figure 11 for the thick spring with $d/R=0.184$ and $\psi=0.13$ versus exact solution. As is seen, these formulae have a very limited range of validity and they are not able to predict any transformations of the roots of the dispersion equation. Dominantly flexural waves (curves 3 and 4) are captured by formulae (3.7*a*) and (3.7*b*) up to $\Omega\approx 0.5\times 10^{-3}$ (returning to dimensional parameters from Lee & Thompson (2001), up to 30 Hz). Dependence of wavenumbers of torsion (3.7*c*) wave (curve 2) and axial (3.7*d*) wave (curve 1) upon frequency is captured somewhat better—up to, roughly speaking, 120 Hz (referring to the case treated in Lee & Thompson (2001)) or $\Omega\approx 0.2\times 10^{-2}$. The validity range of formulae (3.7*a*)–(3.7*d*) may be extended by accounting for higher order terms, but the asymptotic formulae reported in §3*a*,*b* are superior to formulae (3.7*a*)–(3.7*d*) because they present the dominant balances in the dispersion equation.

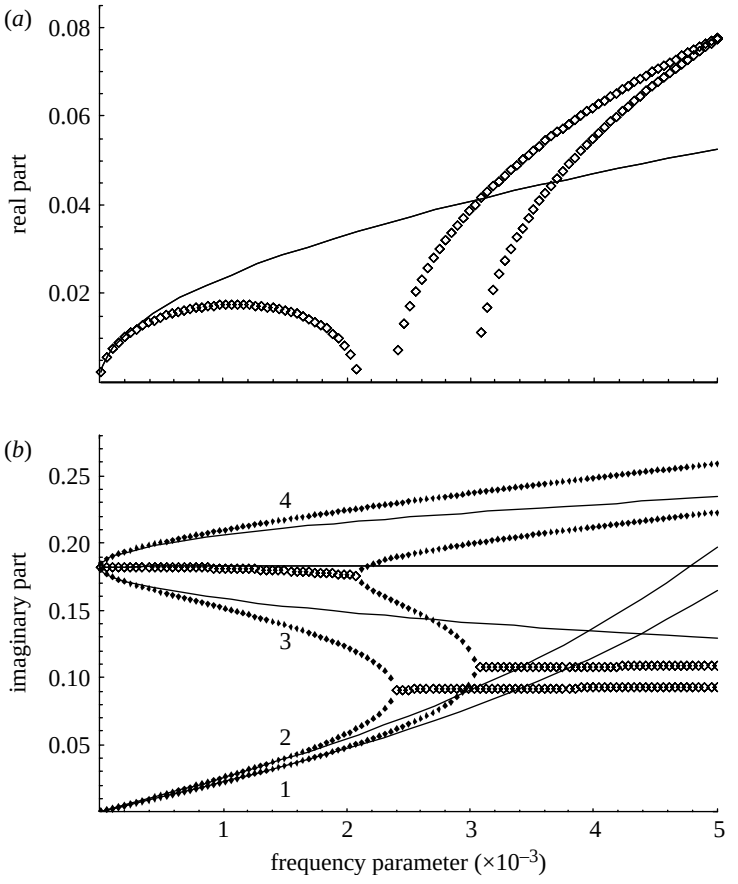

Figure 11. Quasi-static asymptotic of dispersion curves for a 'thick' spring, $d/R=0.184$ and $\psi=0.13$. (*a*) Real and (*b*) imaginary parts of wavenumbers. Symbols are the same as defined in legend of figure 3.

4. Identification of types of waves: analysis of eigenmodes

In the two significant regimes of wave motion explored in §3, it is expedient to identify types of waves associated with each branch of dispersion curves. This is, in effect, the analysis of eigenmodes. As a starting point, it is helpful to refer to the limit case of a circular ring ($\psi=0$). Then, two uncoupled sets of eigenmodes are easily identified: the in-plane waves, which involve the in-plane flexural displacement u coupled with the axial displacement w, and out-of-plane waves, which involve the out-of-plane flexural displacement v coupled with the torsion angle γ. Accordingly, modal coefficients should be introduced in different waves for each type of waves. For in-plane modes, they may be defined as the ratio of the amplitude of the flexural displacement u to the amplitude of the axial displacement w, $\alpha^u_{jw} \equiv U_j/W_j$. In the case $\psi=0$, two other similarly defined modal coefficients vanish: $\alpha^v_{jw} \equiv V_j/W_j = 0$ and $\alpha^\gamma_{jw} \equiv \Gamma_j/W_j = 0$. For out-of-plane modes, they may be defined as the ratio of the amplitude of the torsion angle of cross section γ to the amplitude of the flexural displacement v (scaled

by the diameter of the coil), $\alpha^{\gamma}_{jv} \equiv \Gamma_j / V_j$. Clearly, $\alpha^{u}_{jv} \equiv U_j / V_j = 0$ and $\alpha^{w}_{jv} \equiv W_j / V_j = 0$ in the case $\psi = 0$. The analysis of the types of modes in this degenerate case has been performed by Wittrick (1966), and, here, the coupling between these two sets of waves is studied for the non-zero pitch angle.

This is a relatively simple task in the high-frequency range, as the structure of the asymptotic formulae (3.2*c*), (3.2*d*), (3.3*a*) and (3.3*b*) clearly indicates the dominant type of deformation. Specifically, in the dominantly torsion wave (3.2*c*), see curve 2 in figure 7*b*, the scaled amplitudes of all three translational displacements are much smaller than the amplitude of rotation already at around its cut-on frequency, $|\alpha^{\gamma}_{9v}| \gg 1$, $|\alpha^{u}_{9v}| \ll 1$, $|\alpha^{w}_{9v}| \ll 1$. The dominance of the axial displacement component in the wave (3.2*d*) shown as curve 1 in figure 7*b* gradually develops as the frequency increases. Around its cut-on frequency, the magnitudes of modal coefficients satisfy the following inequalities: $|\alpha^{u}_{11w}| > 1$; $|\alpha^{v}_{11w}| \ll 1$; and $|\alpha^{\gamma}_{11w}| \ll 1$. The two high-frequency flexural waves ((3.3*a*) and (3.3*b*)), see curves 3 and 4 in figure 7*b*, have modal coefficients of displacement components of almost the same magnitude $|\alpha^{u}_{jw}| \sim |\alpha^{v}_{jw}| > 1$. The difference between them is controlled by the phases, which ensure their orthogonality. On balance, it can be concluded that, at high frequencies, axial and torsion waves decouple rather clearly, whereas flexural waves (quasi-in-plane and quasi-out-of-plane) remain strongly coupled.

In the low-frequency regime, this identification is more difficult. Inasmuch as the refined Bernoulli–Euler theory is shown to be accurate to describe wave motion in a helical spring in the low-frequency range, the eigenmodes' analysis is reliably based on equations (3.5) and (3.6*a*)–(3.6*b*). As follows from these formulae, the coupling between all four types of deformation of a coil is essential. It is illustrated here for the thick spring with a relatively small pitch angle, $d/R = 0.184$, $\psi = 0.13$, in the low-frequency range. An inspection into the eigenmodes is performed for four propagating waves, designated in figure 11 as branches 1–4. Branch 1 represents an axial wave (macroscopic torsion of the spring). The dominant component of the displacement is the axial one (figure 1). Already at vanishingly small frequencies, the coupling between quasi-in-plane and quasi-out-of-plane motion is essential—the amplitude ratio $|\alpha^{v}_{1w}|$ is larger than $|\alpha^{u}_{1w}|$. Branch 2 represents a torsion wave (macroscopic elongation/shortening of the spring). The dominant component of displacement is the out-of-plane one and the dominant coupling is between axial and quasi-out-of-plane displacements, as seen from the inequalities: $|\alpha^{w}_{2v}| > |\alpha^{u}_{2v}| > |\alpha^{\gamma}_{2v}|$. Moreover, in the static limit, the following equality holds true: $|\alpha^{v}_{1w}| = |\alpha^{w}_{2v}|$. It means that, at $\Omega = 0$, branch 1 describes rigid body rotation of a spring around its symmetry axis, while branch 2 describes its rigid body motion along the symmetry axis. In both flexural waves (branches 3 and 4 in figure 11), the dominant displacement component is along the axis of wire. All modal coefficients are of the same order of magnitude and it is impractical to trace waves to their in-plane and out-of-plane origins, as suggested by Wittrick (1966).

The strong coupling of all components of displacements in the low-frequency regime of wave motion in a helical spring explains the challenge in the description of waves of axial deformation and torsion below their cut-on, reported in §3. Indeed, the scaling applied to describe dominantly axial and torsion waves in both frequency ranges is defined by setting $n = j$ in formulae (3.1*b*) and (3.1*c*), whereas for dominantly flexural waves, the relation between

powers in leading order terms of asymptotic expansions (3.1*b*) and (3.1*c*) is $n=(1/2)j$. As seen from §3, dominantly flexural waves are captured accurately in both frequency ranges. There are no difficulties in overlapping of asymptotic formulae, because low-frequency flexural waves remain flexural at high frequencies. By contrast, high-frequency axial and torsion waves emerge from low-frequency flexural ones, i.e. the ratio $n=(1/2)j$ is being gradually replaced by the ratio $n=j$ as the frequency grows. This transition occurs in the zone where dispersion curves predicted by formulae (3.2*c*) and (3.2*d*) cross each other. As already mentioned in §3*d*, an inspection into the fine details of the location of the dispersion curves in this particular zone of the (Ω, k) space can be done by means of standard perturbation methods (see Hinch 1991); this issue lies beyond the scope of the present paper.

5. Conclusions

The findings reported in this paper are summarized as follows.

— It is shown that the standard Bernoulli–Euler theory fails to correctly predict the location of dispersion curves and, therefore, should not be used for analysis of dynamics of helical springs.
— The Timoshenko theory should be used in the high-frequency range to correctly describe dominantly flexural waves. Corrections introduced by this theory become significant in the same frequency range as for the straight beams of the given diameter of cross section.
— The refined Bernoulli–Euler theory is valid for analysis of dynamics of helical springs, with the exception of high-frequency dominantly flexural waves.
— All dispersion curves may be adequately described by asymptotic formulae derived by the dominant balance method in low- and high-frequency ranges. There is one narrow zone in the (Ω, k) space where a finer methodology to capture the veering phenomenon has to be applied.
— At low frequencies, the eigenmodes of wave motion involve all displacement components equally, and it is impractical to trace them back to the eigenmodes in a circular ring, whereas, at high frequencies, they gradually recover the structure of the eigenmodes in a straight beam.

As discussed in §1, the obvious continuation of the analysis of wave propagation reported in this paper is a formulation of Green's matrix and of boundary integral equations for helical springs, which would facilitate studies of energy flows in various excitation conditions and reliable prediction of the eigenfrequencies of springs of a finite length.

References

Becker, L. E., Chassie, G. G. & Cleghorn, W. L. 2002 On the natural frequencies of helical compression springs. *Int. J. Mech. Sci.* **44**, 825–841. (doi:10.1016/S0020-7403(01)00096-0)

Chidamparam, P. & Leissa, A. W. 1993 Vibration of planar curved beams, rings and arches. *Appl. Mech. Rev.* **46**, 467–483.

Guido, A. R., Della Pietra, L. & Della Valle, S. 1978 Transverse vibrations of cylindrical helical springs. *Meccanica* **13**, 90–108. (doi:10.1007/BF02128537)

Hinch, E. J. 1991 *Perturbation methods*. Cambridge, UK: Cambridge University Press.

Jiang, W., Wang, T. L. & Jones, W. K. 1992 The forced vibration of helical springs. *Int. J. Mech. Sci.* **34**, 549–562. (doi:10.1016/0020-7403(92)90030-K)

Lee, J. 2007 Free vibration analysis of cylindrical helical springs by the pseudospectral method. *J. Sound Vib.* **302**, 185–196. (doi:10.1016/j.jsv.2006.11.008)

Lee, J. & Thompson, D. J. 2001 Dynamic stiffness formulation, free vibration and wave motion of helical springs. *J. Sound Vib.* **239**, 297–320. (doi:10.1006/jsvi.2000.3169)

Love, A. E. M. 1899 The propagation of waves of elastic displacement along a helical wire. *Trans. Camb. Philos. Soc.* **18**, 364–374.

Mottershead, J. E. 1980 Finite elements for dynamical analysis of helical rods. *Int. J. Mech. Sci.* **22**, 267–283. (doi:10.1016/0020-7403(80)90028-4)

Pearson, D. & Wittrick, W. H. 1986 An exact solution for vibration of helical springs using a Bernoulli–Euler model. *Int. J. Mech. Sci.* **28**, 263–284. (doi:10.1016/0020-7403(86)90016-0)

Phillips, W. & Costello, G. A. 1972 Large deflections of impacted helical springs. *J. Acoust. Soc. Am.* **51**, 967–973. (doi:10.1121/1.1912946)

Shames, I. H. & Dym, C. L. 1991 *Energy and finite element methods in structural mechanics*. New York, NY: Taylor & Francis.

Sorokin, S. V. 2008*a* Linear wave motion in elastic helical springs—revisited. In *Proc. 15th Int. Congress on Sound and Vibration Daejeon, Korea, 6–10 July 2008* (ed. Ch.-W Lee). CD-ROM proceedings ISBN 978-89-96084-1-0-98060

Sorokin, S. V. 2008*b* Asymptotic analysis of linear wave propagation in and free vibration of elastic helical springs. In *Proc. 22nd Int. Congress of Theoretical and Applied Mechanics Adelaide, Australia, 24–29 August 2008* (eds J. Denier, M. D. Finn & T. Mattner). CD-ROM proceedings ISBN 978-0-9805142-1-6

Sorokin, S. V. & Peake, N. 2006 On symmetry-breaking effects in propagation of waves in sandwich plates with and without heavy fluid loading. *J. Sound Vib.* **295**, 114–128. (doi:10.1016/j.jsv.2005.12.055)

Telem, B., Calim, F. F. & Tutuncu, N. 2004 Quasi-static and dynamic response of visco-elastic helical rods. *J. Sound Vib.* **271**, 921–935. (doi:10.1016/S0022-460X(03)00760-0)

Treysséde, F. 2008 Elastic waves in helical waveguides. *Wave Motion* **45**, 457–470. (doi:10.1016/j.wavemoti.2007.09.004)

Wittrick, W. H. 1966 On elastic wave propagation in helical springs. *Int. J. Mech. Sci.* **8**, 25–47. (doi:10.1016/0020-7403(66)90061-0)

Wolfram, S. 1991 *Mathematica: a system for doing mathematics by computer*. Reading, MA: Addison-Wesley Publishing Co.

Yildirim, V. 1996 Investigation of parameters affecting free vibration frequency of helical springs. *Int. J. Numer. Meth. Eng.* **39**, 99–114. (doi:10.1002/(SICI)1097-0207(19960115)39:1<99::AID-NME850>3.0.CO;2-M)